

Free Radical-Mediated Heterogeneous Photocatalytic Reduction of Metal Ions in UV-Irradiated Titanium Dioxide Suspensions

Sashikala Somasundaram, Yong Ming, C. R. Chenthamarakshan, Zoltan A. Schelly, and Krishnan Rajeshwar*

Department of Chemistry and Biochemistry, The University of Texas at Arlington, Arlington, Texas 76019-0065

Received: September 12, 2003; In Final Form: February 17, 2004

This paper describes the indirect photocatalytic reduction of four metal ions: Cd^{2+} , Zn^{2+} , Mn^{2+} , and Tl^+ using formate radical anions ($\text{CO}_2^{\bullet-}$) generated in UV-irradiated aqueous TiO_2 suspensions. Trends in the reactivity of these four metal ions are compared with corresponding rate constants reported in the literature for the homogeneous reactions of these metal ions with $\text{CO}_2^{\bullet-}$ in aqueous media. In both cases, the reaction rates follow the same order: $\text{Cd}^{2+} > \text{Tl}^+ > \text{Mn}^{2+} > \text{Zn}^{2+}$. Using Tl^+ as a model metal ion, a simple kinetics scheme is developed for the indirect reduction route, and the predictions from this model are shown to be in excellent agreement with experimental data.

Introduction

Heterogeneous photocatalysis using UV-irradiated titanium dioxide (TiO_2) suspensions or films in aqueous media, is now a mature field.^{1–6} The photocatalytic reduction of metal ions in such media has both fundamental and practical interest.^{1,7} While metal ions with rather positive standard reduction potentials [i.e., positive of 0 V versus the standard hydrogen electrode reference (SHE), see ref 8] such as Cu^{2+} , Cr^{6+} , Au^{3+} , Ag^+ , etc., have been widely investigated, only a few studies exist on metal ions that are much more difficult to be reduced, for example: Cd^{2+} , Zn^{2+} , Mn^{2+} , Tl^+ .⁸ In this paper, we consider the photocatalytic reduction of these four species using organic free radicals that are photogenerated at the TiO_2 /water interface. Formate was used as the reducing agent (i.e., free radical source) in this study.

Initial photoexcitation of TiO_2 creates electron–hole pairs, some of which escape recombination and diffuse to the oxide/water interface.^{2,3} There they encounter electron acceptors (e.g., H^+ , O_2) or electron donors (formate ions, OH^- , water molecules). The photooxidation of formate (either directly by the photogenerated holes or via the intermediacy of OH^{\bullet}) generates the formate radical anion, $\text{CO}_2^{\bullet-}$. While this species is well-known to be strongly and quantitatively reducing toward a variety of organic and inorganic compounds, there is some uncertainty in the value for the standard reduction potential of $\text{CO}_2^{\bullet-}$ on the SHE scale.⁹ Taking a value of -1.90 V,¹⁰ however, Figure 1 shows that $\text{CO}_2^{\bullet-}$ is thermodynamically capable of reducing all four metal ions considered in this study, namely Cd^{2+} , Zn^{2+} , Mn^{2+} , and Tl^+ . On the other hand, the *direct* reduction of $\text{Mn}(\text{II})$ and $\text{Zn}(\text{II})$ by the electrons photogenerated in TiO_2 is thermodynamically prohibited (Figure 1). [We assume for this discussion that we are only dealing with thermalized (i.e., not “hot”) electrons at the oxide/water interface]. By the same token, the direct photocatalytic reduction of $\text{Cd}(\text{II})$ and $\text{Tl}(\text{I})$ has only a modest driving force (Figure 1). Experimental data are fully in agreement with these thermodynamic predictions.⁸

As mentioned earlier, only a few studies exist on the *indirect* photocatalytic reduction of metal ions using free radicals

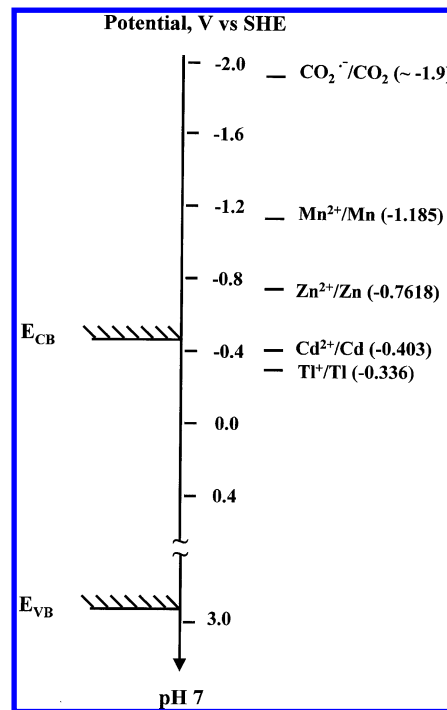


Figure 1. Relative disposition of the energy levels in TiO_2 and solution species. A pH of 7 was assumed for this interfacial situation; see discussion in the text.

generated on oxide semiconductor surfaces under UV illumination. Free radicals derived from formate or ethanol were shown to enhance the photoreduction of *p*-nitrosodimethylaniline in UV-irradiated ZnO aqueous suspensions.¹¹ Photodeposition of Pt, Ag, and Au was performed on a positively biased TiO_2 electrode in an aqueous solution containing radical intermediates derived from alcohols.¹² Nickel(II) was photoreduced by $\text{CO}_2^{\bullet-}$ generated from the initial photooxidation of oxalate ions in UV-irradiated TiO_2 suspensions.¹³ In our own laboratory, the free radical-mediated indirect photocatalytic reduction route has been demonstrated for a variety of species: $\text{Ni}(\text{II})$,¹⁴ $\text{Pb}(\text{II})$,¹⁵ $\text{As}(\text{V})$,¹⁶ $\text{Zn}(\text{II})$,^{8,17,18} $\text{Cd}(\text{II})$,^{8,17,18} $\text{Mn}(\text{II})$,^{8,19} and $\text{Tl}(\text{I})$ ^{8,20} in UV-irradiated TiO_2 suspensions.

* To whom correspondence should be addressed. E-mail: rajeshwar@uta.edu.

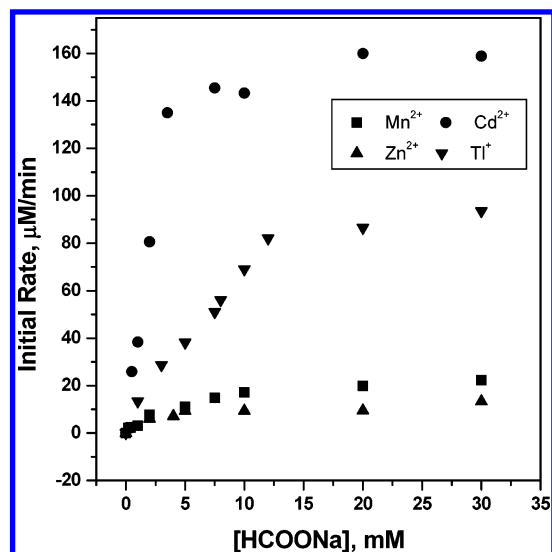


Figure 2. Dependence of the initial rate of metal ion photoreduction on the formate additive concentration in UV-irradiated TiO₂ suspensions. The initial concentration of the metal ion (added as the sulfate salt) was 200 μM.

In the present study, we consider this indirect route in much more detail than in the prior studies referenced above. Specifically, we consider the importance of metal ion adsorption on the TiO₂ surface and also compare the heterogeneous photo-reactivity trends for the four species [Cd(II), Zn(II), Mn(II), and Tl(I)] with the corresponding rate constants reported in the literature for the homogeneous reactions of these metal ions with CO₂^{•-} in aqueous media. Finally, a simple kinetics scheme is developed for the indirect reduction route, and the predictions from this model, are shown to be in excellent agreement with experimental data.

Experimental Section

Chemicals. Zinc sulfate (Aldrich, 99%), cadmium sulfate (Aldrich, 98%), thallium sulfate (Johnson Matthey, 99.9%), and manganese sulfate (Fisher, 99.2%) were used without further purification. Sodium formate (99%) was from Alfa Aesar and was used without further purification. The TiO₂ (Degussa P-25) used was predominantly anatase and had a specific surface area of ~60 m²/g. Deionized water (18 MΩ) was used in all cases for preparing solutions or suspensions (unless otherwise specified).

Instrumentation and Procedures. In all the experiments the TiO₂ suspension dose was 2 g/L; the suspensions were agitated by sparging ultrapure N₂ through them. All measurements pertain to the laboratory ambient temperature (25 ± 5 °C). The photoreactor used was described previously.²¹ The light source was a 400 W medium-pressure Hg arc lamp (Philips).

For obtaining the data presented in Figure 2, the initial concentrations of the metal ions (Cd²⁺, Zn²⁺, Mn²⁺, and Tl⁺) in all cases were 200 μM. Prior to UV irradiation, the metal ion and sodium formate additive (ranging in concentrations from 1 to 30 mM) loaded TiO₂ suspensions were equilibrated in the dark for 30 min. Procedures for aliquot withdrawal and determination of metal ion concentration have been described previously.^{8,17,18} Manganese, cadmium, and thallium ion concentrations in solution were determined by flame atomic absorption spectrometry (FAAS) at 279.5, 228.8, and 276.8 nm, respectively. Zn(II) concentrations in solution were determined by UV-Vis spectrophotometry at 492 nm after derivatizing with 4-(2-pyridylazo)-resorcinol.^{17,18}

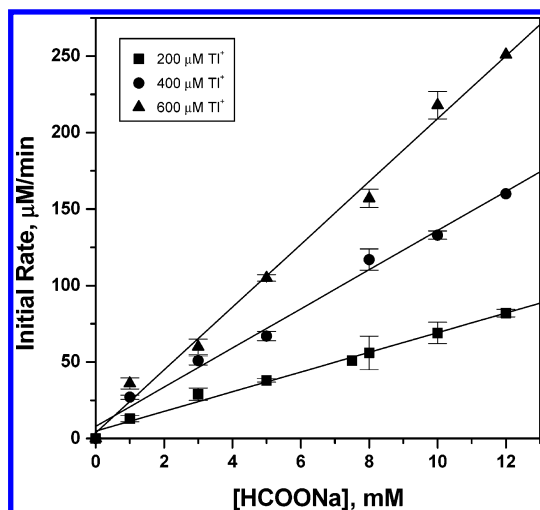


Figure 3. Test of the model prediction (represented by eq 10) for three initial concentrations of Tl(I). Other conditions are described in the Experimental Section. The lines are least-squares fits and the error bars are shown for cases where replicate experiments were performed.

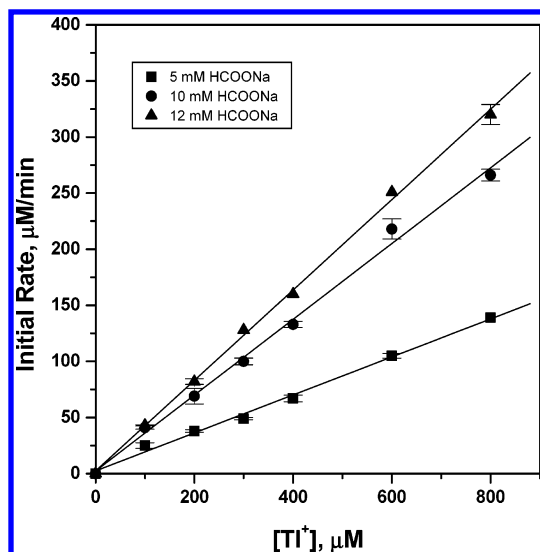


Figure 4. As in Figure 3 but for the set of experiments where Tl(I) concentration was varied while holding the formate concentration constant at the three values shown.

A more detailed set of experiments were performed on the Tl(I) system for testing against the kinetics model. Thus, unlike the procedure that led to Figure 2 where only a single metal ion concentration (200 μM) was utilized, runs were done at three initial concentrations of Tl(I) (200 μM, 400 μM, and 600 μM) in the TiO₂ suspensions containing variable amounts of formate in the 1–12 mM range (Figure 3). Alternatively, the formate concentrations were fixed at 5 mM, 10 mM, and 12 mM, respectively, and the Tl(I) ion concentration was systematically varied in the 100–800 μM range to generate the set of data in Figure 4.

UV-Vis spectrophotometry employed a Hewlett-Packard model HP 8452 diode array spectrometer. FAAS was performed on a Perkin-Elmer 2380 atomic absorption spectrometer.

Results and Discussion

Trends in Photoreactivity and Dark Adsorption. Figure 2 contains plots of the initial reaction rate versus the formate additive concentration ($[D^-]_0$) for the four metal ions considered in this study. The initial rate was determined as usual from the

TABLE 1: Rate Constants^a for the Homogeneous and Heterogeneous Reactions between Metal Ions and Formate Radicals

metal ion	homogeneous, ^b k (L mol ⁻¹ s ⁻¹)	heterogeneous, ^c $k'k''$ (L mol ⁻¹ s ⁻¹)
Cd ²⁺	5.1×10^6	3.2
Zn ²⁺	$< 2 \times 10^4$	0.14
Mn ²⁺	$< 2 \times 10^5$	0.15
Tl ⁺	3×10^6	0.55

^a From ref 23. ^b Single electron transfer in all cases; see text. ^c See text and eq 10 for details.

slopes of reactant conversion plots of metal ion concentration versus time. In all four cases, the initial rate rapidly increases with $[D^-]_0$ in a roughly linear fashion and then attains a plateau. The rates were ordered as follows: $Cd^{2+} \gg Tl^+ > Mn^{2+} > Zn^{2+}$. It must be noted that the photocatalytic conversion rates are either zero (Mn^{2+} , Zn^{2+}) or negligible (Cd^{2+} , Tl^+) in the absence of the formate additive.⁸ Thus the data in Figure 2 predominantly reflect trends in the radical-mediated indirect conversion route. It is also worth noting that the ratio $[D^-]_0/[M^{n+}]_0$ (where $[M^{n+}]_0$ = initial metal ion concentration) far exceeds unity in *all* the experiments pertinent to Figure 2. This point is amplified in a subsequent section.

Since the band-edge positions of TiO_2 in the solution and some solution processes (e.g., acid–base equilibria) are dependent on solution pH, considerable attention was focused on this parameter. All the experiments in this study were performed at the “natural” pH range of the oxide and metal ion/additive laden suspensions, namely ~ 6.5 – 7.0 . The use of pH buffers was avoided because of possible interference of the buffer agent components with the oxide surface and/or the photocatalytic process. The pH values of the solutions were also monitored during the photocatalytic process; they did not change by more than 0.2 units. This is within the experimental error; note also that only the *initial* reaction rates were relevant for the purposes of this study. Thus the reaction timespan did not exceed 5 min in all the cases. The band-edge positions in Figure 1 are relevant for a solution pH of ~ 7.0 , and it is also worth noting that since the pK_a of $HCOO^\bullet$ is ~ 2.3 ,²² almost all the radical species will be in the dissociated state.

It is of interest to compare the reactivity trends in Figure 2 with the corresponding trends for the *homogeneous* reactions of the metal ions with $CO_2^{\bullet-}$ radicals. Bimolecular rate constants for the homogeneous (one-electron transfer) reactions are available in the literature;²³ Table 1 lists these values. The rate constants broadly follow the same order: $Cd^{2+} > Tl^+ > Mn^{2+} > Zn^{2+}$, as observed in the heterogeneous case. The rate constants for the heterogeneous reactions (see below) are also listed in Table 1.

One could argue that initial adsorption of the metal ion (and the formate additive) on the TiO_2 surface could play an important role in a heterogeneous photoreaction environment. We have shown earlier⁸ that, in the absence of formate, the proclivity of these metal ions to adsorb on the TiO_2 surface is quite low but varies among the four species considered. On the other hand, *induced* adsorption (on the TiO_2 surface) results when chelating additives such as formate are present.^{17,18} Possible mechanistic factors underlying this interesting trend have been discussed both by us^{17,18} and by other authors.²⁴ Table 2 contains the dark adsorption data for the four metal ions. In the presence of formate (the situation corresponding to the experiments addressed in Figure 2), the adsorption affinity follows the order: $Zn^{2+} \approx Cd^{2+} > Tl^+ > Mn^{2+}$. Clearly, for Cd^{2+} , Tl^+ , and Mn^{2+} , this trend parallels that seen earlier in

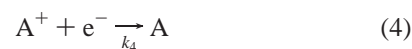
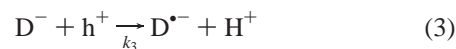
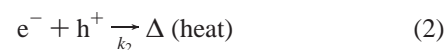
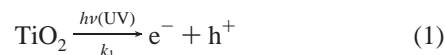
TABLE 2: Amount of Metal Ion Adsorbed on the TiO_2 Surface with and without Formate Ions Present^a

metal ion ^b	amount adsorbed (μM)	
	with formate ^c	without formate ^d
Cd ²⁺	100	11.1
Zn ²⁺	110	32.6
Mn ²⁺	80	5.6
Tl ⁺	50	20

^a See Experimental Section for details on how adsorption was quantified. ^b Initial concentration was 200 μM in all the cases. ^c Formate concentration was 0.05 M except for Mn^{2+} where it was 0.15 M. ^d From refs 18,19, 26.

Figure 2 and Table 1. On the other hand, the situation with Zn^{2+} shows that interfacial adsorption alone is not a determining factor in the efficacy of its photocatalytic conversion in the presence of the formate additive.

The Thallium(I) Model System: Kinetics Scheme and Comparison with Experimental Data. Given that the photocatalytic (reductive) conversion of $Tl(I)$ species involves a one-electron-transfer situation, a simple reaction scheme can be written for the indirect radical-mediated reaction route:



In the above scheme, the k 's are the rate constants, D^- is an electron donor (formate in our case), A^+ is an electron acceptor (e.g., H^+), M^+ is a metal ion (e.g., Tl^+), and X is a $D^{\bullet-}$ scavenger (e.g., H^\bullet , OH^\bullet , or TiO_2). It is reasonable to assume that $[X] \gg [D^{\bullet-}]$. Thus step (6) can be treated as a pseudo-first-order reaction, with a rate constant, $k_6 = k_6'[X]$.

Invoking the steady-state approximation for the formate radical anion,

$$k_3[D^-][h^+] = k_5[D^{\bullet-}][M^+] + k_6[D^{\bullet-}] = [D^{\bullet-}]\{k_5[M^+] + k_6\}$$

we obtain its concentration as

$$[D^{\bullet-}] = \frac{k_3[D^-][h^+]}{k_5[M^+] + k_6} \quad (7)$$

Thus by assuming reaction 5 to be the rate-determining step, the rate R for the reduction of the metal ion by the radical anion can be written as

$$R_5 = k_5[D^{\bullet-}][M^+] \quad (8)$$

which, after substitution of eq 7, yields

$$R_5 = \frac{k_3 k_5 [D^-][h^+][M^+]}{k_5 [M^+] + k_6} \quad (9)$$

Considering the situation when $k_6 \gg k_5[M^+]$, eq 9 simplifies to

$$R_5 = \frac{k_3 k_5}{k_6} [D^-][h^+][M^+]$$

which can be written as

$$R_5 = k'k''[D^-][M^+] \quad (10)$$

with $k' = k_3[h^+]$ and $k'' = k_5/k_6$.

Equation 10 affords a route to testing this simple kinetics model against experimental data. Thus, the initial rate can be plotted against the initial concentration of formate ($[D^-]_0$) with $[M^+]_0$ held constant. Similar plots can be constructed from experiments with $[M^+]_0$ varied while maintaining $[D^-]_0$ constant. The two sets of plots should result in straight lines, and from their slopes, the product $k'k''$ can be computed. An important test for the efficacy of the present model is that the values obtained for $k'k''$ from the two sets of experiments should be the same, within experimental error.

Figure 3 displays plots of eq 10 generated from experiments where the initial formate ion concentration was varied, while maintaining the initial Tl⁺ concentration constant at three different values. It must be noted, with respect to the Tl⁺ data in Figure 2, that the formate ion concentrations (1–12 mM) were varied within the “linear” rate regime, i.e., not in the saturation region. As the counterpart for these sets of experiments, the Tl⁺ ion concentration was varied for Figure 4. Most of the data points in Figures 3 and 4 are averaged values obtained from replicate (2–3) experiments so that the six plots are built from a cumulative total of 60 runs in all. The lines in Figures 3 and 4 are least-squares fits to the data points. Table 3 lists the six values of $k'k''$ thus obtained from the slopes of the corresponding plots in Figures 3 and 4. These values are clearly in good accord with one another within the data scatter and experimental error, which are further elaborated below.

General Discussion

Trends in the reactivity of four metal ions [Cd²⁺, Zn²⁺, Mn²⁺, and Tl⁺] to undergo free radical-mediated heterogeneous photocatalytic reduction in UV-irradiated TiO₂ suspensions have been presented in this study. These metal ions either have more negative standard reduction potentials or lie very close to the TiO₂ conduction band edge (Figure 1) such that the direct reduction route involving photogenerated electrons in TiO₂ can be neglected. The good correspondence of the present data with the reactivity trends for these same four metal ions in homogeneous media (Table 1) suggests that the dominant role of TiO₂ is as a source of the free radicals. Indeed, interfacial adsorption does not appear to be an overriding factor, at least under the experimental conditions utilized in this study (also see below).

It is also worth noting that the literature kinetics data in Table 1 pertain to single-electron-transfer processes. On the other hand, the results in Figure 2 involve two-electron-transfer processes with the exception of the Tl⁺ case. Nonetheless, it would appear, from the similarity in trends in the two cases, that the rate-determining step is the same in both the homogeneous and heterogeneous processes. In this regard, it is worth noting that the rate constants in homogeneous media for the transfer of the

TABLE 3: Values of $k'k''$ (eq 10) from the Slopes of the Plots in Figures 3 and 4

parameter	$k'k''$ (L mol ⁻¹ s ⁻¹)	r^2 ^a
[Tl ⁺] = 200 μM (Figure 3)	0.53	0.993
[Tl ⁺] = 400 μM (Figure 3)	0.53	0.990
[Tl ⁺] = 600 μM (Figure 3)	0.57	0.990
	avg: 0.54 (±0.02)	
[HCOONa] = 5 mM (Figure 4)	0.565	0.999
[HCOONa] = 10 mM (Figure 4)	0.563	0.995
[HCOONa] = 12 mM (Figure 4)	0.562	0.995
	avg: 0.563 (±0.001)	

^a Correlation coefficient in the least-squares regression.

second electron is orders of magnitude higher than the first step, e.g., 5.1×10^6 L mol⁻¹ s⁻¹ for Cd²⁺ → Cd⁺ versus 2×10^9 L mol⁻¹ s⁻¹ for Cd⁺ → Cd⁰, ref 23. This is entirely consistent with the relative stabilities of the metal ions in the two oxidation states.

A simple kinetics scheme was developed and experimentally tested for the first time for the free radical-mediated (indirect) reduction route. Thallium(I) was used as the metal ion candidate for reaction with the photogenerated formate radicals for this purpose. In a historical sense, it is interesting to note that the Tl⁺_{aq}/Tl⁰ redox couple has been previously utilized for estimation of the reduction potentials of CO₂^{•-} and the alcohol radicals.^{9,10,25} These prior studies in homogeneous media utilized pulse radiolysis for free radical generation. The excellent agreement between our model predictions and experimental data (Table 3, Figures 3 and 4) suggests that the simple scheme represented by eqs 1–6 accounts for the essential aspects of the indirect metal ion reduction route in UV-irradiated TiO₂ suspensions and that thallium(I) is a good model for the heterogeneous system as well.

Several points regarding our kinetics scheme deserve further discussion. Thus, the role of the electron acceptor in scavenging the photogenerated electrons in TiO₂ (eq 4) is not specifically addressed herein. The two possible sinks for electrons are H⁺ ions in solution (or at the interface) and the TiO₂ surface itself. Evidence for the participation of H⁺ ions was found in our earlier study on the photocatalytic reduction of Mn²⁺ species.¹⁹ Charging of the TiO₂ surface by the photogenerated electrons and subsequent trapping of the latter (i.e., Ti(IV)–OH + e⁻ → Ti(III)–OH) can be directly monitored in chronopotentiometric experiments under oxide illumination.²⁶

While our first-generation kinetics scheme (eqs 1–10) is undoubtedly simplified, the possible complicating role of other solution processes such as radical dimerization (as pointed out by a reviewer), can be discounted. For example, the dimerization of CO₂^{•-} occurs only at pH values higher than ~ 8.1.²⁷ Other processes consuming the radicals, such as disproportionation, are mechanistically accommodated by eq 6 in our scheme.

Under steady-state conditions, the electron and hole fluxes on each (irradiated) TiO₂ particle in the suspension must balance one another.²⁸ Furthermore, the assumption leading to eq 10 from eq 9 merits scrutiny. The condition $k_6 \gg k_5[M^+]$ is consistent with the typically high rate of radical annihilation steps (such as reaction 6) in the overall scheme. Indeed, this is consistent with our experimental observation that a large excess of the electron donor (i.e., the free radical source) relative to the initial metal ion concentration is needed to sustain a measurable photocatalytic reduction rate. This condition then maximizes the encounter of a given metal ion with a free radical in its immediate vicinity. In this sense, the rate constant k'' (= k_5/k_6) is a “branching ratio” in that it represents the competition between reactions 5 and 6 for consumption of the photogener-

ated free radical ions. It is worth noting that the opposite situation where $k_5 [M^+] \gg k_6$ (see eq 9) would have yielded a final rate expression that does not contain a $[M^+]$ term. This would clearly be in conflict with the experimental data (see Figure 4).

The postulate of TiO_2 as a quencher of the D^{*+} species (see above) deserves comment. It is well-known that oxide electrodes such as TiO_2 act as hosts for electron injection from (unstable) radicals leading to the so-called current-doubling effect.²⁹ This effect is likely to play a role in oxide suspensions as well, so that TiO_2 competes with the metal ions for electrons from the photogenerated formate radical anions.

The plateaus seen in Figure 2 in the initial rates at formate concentrations higher than 5–10 mM are explained as follows. At formate concentrations lower than this regime, the photocatalytic reduction of 200 $\mu M M^{n+}$ ions is radical-limited. At higher concentrations of formate, a proportionately higher concentration of free radicals is generated so that the process is no longer radical-limited and the conversion rate saturates.

Finally, this study has not specifically addressed the location of the reaction zone involving the metal ions and the photo-generated free radical ions. Nevertheless, initial concentrations and initial rates were used in eq 10 for successfully testing the model against the experimental data (Figures 3 and 4). This suggests that interfacial adsorption (of either Tl^+ , formate ion, or both) on the TiO_2 surface exerts only a secondary effect on the overall electron transfer rate. Close examination of the results from analyzing the plots in Figures 3 and 4 (Table 3), however, reveals that the data scatter (and the consequent slope uncertainty) are distinctly higher in the cases where the formate concentrations were systematically varied (Figure 3). This is further borne out by the relative magnitudes of the regression correlation coefficients in the two sets of cases (Table 3). Recalling that formate ions provide the anchoring links for adsorption of Tl^+ (and other metal) ions on the TiO_2 surface,^{17,18,20,28} we attribute this additional data scatter to the perturbation induced by the variable formate levels on the local Tl^+ ion concentrations at the TiO_2 /water interface.

Notwithstanding such subtler effects, the overall kinetics scheme and the simple rate expression in eq 10 do appear to provide a satisfactory description for the free radical-mediated reduction of metal ions in UV-irradiated TiO_2 suspensions. At this stage of our understanding of this interesting process, it is not yet possible to further separate the contributions of the two terms k' and k'' from the measured slopes. Efforts in this direction are planned and fall beyond the scope of the present study.

Acknowledgment. This research was supported, in part, by a grant from the U.S. Department of Energy, Office of Basic Energy Sciences. Z.A.S. thanks The Welch Foundation for support. We thank a reviewer for constructive criticisms of an earlier version of this manuscript.

References and Notes

- (1) Rajeshwar, K. *J. Appl. Electrochem.* **1995**, *25*, 1067.
- (2) Linsebigler, A. L.; Lu, G.; Yates, J. T., Jr. *Chem. Rev.* **1995**, *95*, 735.
- (3) Rajeshwar, K.; Ibanez, J. *Environmental Electrochemistry*; Academic Press: San Diego, 1997.
- (4) Fujishima, A.; Rao, T. N.; Tryk, D. A. *J. Photochem. Photobiol. C: Photochem. Rev.* **2000**, *1*, 1.
- (5) Blake, D. M. Bibliography of Work on the Heterogeneous Photocatalytic Removal of Hazardous Compounds from Water and Air. NREL/TP-570-26797, National Renewable Energy Laboratory: Golden, CO, 1999. Update No. 4 to October 2001, NREL/TP-510-31319.
- (6) Diebold, U. *Surf. Sci. Rep.* **2003**, *48*, 53.
- (7) Litter, M. I. *Appl. Catal. B. Environ.* **1999**, *23*, 89.
- (8) Rajeshwar, K.; Chenthamarakshan, C. R.; Ming, Y.; Sun, W. *J. Electroanal. Chem.* **2002**, *538–539*, 173, and references therein.
- (9) See, for example: Koppenol, W. H.; Rush, J. D. *J. Phys. Chem.* **1987**, *91*, 4429.
- (10) Schwarz, H. A.; Dodson, R. W. *J. Phys. Chem.* **1989**, *93*, 409.
- (11) Cunningham, J.; Zainal, H. *J. Phys. Chem.* **1972**, *76*, 2362.
- (12) Baba, R.; Konda, R.; Fujishima, A.; Honda, K. *Chem. Lett.* **1986**, 1307.
- (13) Forouzan, F.; Richards, T. C.; Bard, A. J. *J. Phys. Chem.* **1996**, *100*, 18123.
- (14) Lin, W.-Y.; Rajeshwar, K. *J. Electrochem. Soc.* **1997**, *144*, 2751.
- (15) Chenthamarakshan, C. R.; Yang, H.; Savage, C. R.; Rajeshwar, K. *Res. Chem. Intermed.* **1999**, *25*, 861.
- (16) Yang, H.; Lin, W.-Y.; Rajeshwar, K. *J. Photochem. Photobiol. A: Chem.* **1999**, *123*, 137.
- (17) Chenthamarakshan, C. R.; Rajeshwar, K. *Electrochem. Commun.* **2000**, *2*, 527.
- (18) Chenthamarakshan, C. R.; Yang, H.; Ming, Y.; Rajeshwar, K. *J. Electroanal. Chem.* **2000**, *494*, 79.
- (19) Ming, Y.; Chenthamarakshan, C. R.; Rajeshwar, K. *J. Photochem. Photobiol. A: Chem.* **2002**, *147*, 199.
- (20) Kajitvichyanukul, P.; Chenthamarakshan, C. R.; Rajeshwar, K.; Qasim, S. R. *J. Electroanal. Chem.* **2002**, *519*, 25.
- (21) Lin, W.-Y.; Rajeshwar, K. *J. Electrochem. Soc.* **1993**, *140*, 2477.
- (22) von Sonntag, C.; Schuchmann, H.-P. *Carbohydrates*. Jonah, C. D., Rao, B. S. M., Eds.; Elsevier: Amsterdam, 2001.
- (23) Neta, P.; Grodkowski, J.; Ross, A. B. *J. Phys. Chem. Ref. Data* **1996**, *25*, 709.
- (24) Rajh, T.; Ostafin, A. E.; Micic, O. I.; Tiede, D. M.; Thurnauer, M. C. *J. Phys. Chem.* **1996**, *100*, 4538.
- (25) Butler, J.; Henglein, A. *Radiat. Phys. Chem.* **1980**, *15*, 603.
- (26) Sun, W.; Chenthamarakshan, C. R.; Rajeshwar, K. *J. Phys. Chem. B* **2002**, *106*, 11531.
- (27) Fojtik, A.; Czapki, G.; Henglein, A. *J. Phys. Chem.* **1970**, *74*, 3204.
- (28) Kajitvichyanukul, P.; Chenthamarakshan, C. R.; Rajeshwar, K.; Qasim, S. R. *Adsorp. Sci. Technol.* **2003**, *21*, 217.
- (29) Morrison, S. R. *The Chemical Physics of Surfaces*; Plenum Press: New York and London, 1977.